

PROCEEDINGS OF SPIE

[SPIDigitalLibrary.org/conference-proceedings-of-spie](https://spiedigitallibrary.org/conference-proceedings-of-spie)

Towards freeform curved blazed gratings using diamond machining

C. Bourgenot, D. J. Robertson, D. Stelter, S. Eikenberry

C. Bourgenot, D. J. Robertson, D. Stelter, S. Eikenberry, "Towards freeform curved blazed gratings using diamond machining," Proc. SPIE 9912, Advances in Optical and Mechanical Technologies for Telescopes and Instrumentation II, 99123M (22 July 2016); doi: 10.1117/12.2231182

SPIE.

Event: SPIE Astronomical Telescopes + Instrumentation, 2016, Edinburgh, United Kingdom

Towards freeform curved blazed gratings using diamond machining

C. Bourgenot^a, D. J. Robertson^a, D. Stelter^b and S. Eikenberry^b

^aDurham University, Department of Physics, Centre for Advanced Instrumentation, NETPark Research Institute, Joseph Swan Road, Sedgefield, TS21 3FB, UK;

^bUniversity of Florida, Department of Astronomy, 211 Bryant Space Science Ctr., Gainesville, FL 32611-2055, USA;

ABSTRACT

Concave blazed gratings greatly simplify the architecture of spectrographs by reducing the number of optical components. The production of these gratings using diamond-machining offers practically no limits in the design of the grating substrate shape, with the possibility of making large sag freeform surfaces unlike the alternative and traditional method of holography and ion etching. In this paper, we report on the technological challenges and progress in the making of these curved blazed gratings using an ultra-high precision 5 axes Moore-Nanotech machine. We describe their implementation in an integral field unit prototype called IGIS (Integrated Grating Imaging Spectrograph) where freeform curved gratings are used as pupil mirrors. The goal is to develop the technologies for the production of the next generation of low-cost, compact, high performance integral field unit spectrometers.

Keywords: Diamond turning, tool servo, freeform optics, precision machining

1. INTRODUCTION

Nowadays, curved gratings are used in a large number of spectrometers architecture^{1,2} for their capacity to both disperse the light and reimage the slit at the same time. Concave gratings are most common and enable much more compact spectrometers compared to other architectures such as Czerny-Turner configuration.³ Convex gratings on the other hand, are less in use but can nonetheless offer a substantial flexibility in design such as in an Offner type configuration.⁴ Curved blazed grating, which significantly improves efficiency by superimposing on the surface a faceted saw-tooth shape grooves are generally made by holographic exposure method followed by an ion beam etching technology on a photoresist⁵ or directly engraved with a V shape diamond tool in a metallic substrate. Holographic techniques offer a wide range of advantages.⁶ Most importantly being the fact that the gratings are produced with almost no random or periodic errors, resulting in minimum stray light.⁷ However, when it comes to producing blazed grating by way of holography, the creation of the grooves by ion etching technologies or electron beam lithography requires a complex set-up. Although diamond machined gratings cannot yet compete with holographic ones in term of stray light, they appear to be ideal candidates for systems where the mechanical properties of the substrate is imposed for the purpose of athermalization for example, and/or for use in harsher environmental conditions where the photoresist is not an option. Similarly, because ultra-precision 5 axis machines have practically no limitations in the production of the substrates form, with the possibility of generating high sag with steep slopes surfaces, gratings produced by diamond machining become a cost effective and viable alternative.⁸ Finally, one of their most important benefits is the ability to control the groove profiles in a well-defined manner. Because the grating's efficiency is determined by the quality of the groove profile, ruled gratings, including diamond machined ones, usually show better efficiency than holographic ones.⁶ In this paper, we report on the first design and machining of an integral field unit spectrometer using diamond machined curved grating. The system called IGIS (Integrated Grating Imaging Spectrograph) has been designed by the University of Florida for remote sensing applications and the University of Durham has taken over both the machining and assembly.

Further author information: (Send correspondence to cyril.bourgenot@durham.ac.uk)

The intensity distribution at the image plane of a telescope is sliced and reformatted into a slit by a combination of slicer and pupil mirrors arrays. The pupil mirrors, which are concave gratings, also disperse the slit-like object into a spectrum allowing a very compact design. In the first part of the paper, we compare the performance in terms of image quality, of 2 types of grating with similar dimensions and working conditions. One is a sphere and the other is an ellipse, and both work in a point conjugate configuration. This configuration is to the one in IGIS. Particular attention is given to how the definition of the groove pitch affects the performance. In the second part, we describe the optical design of IGIS and give some preliminary results on a test sample representative of the spherical pupil mirror. In the third and last section, we discuss how IGIS resolving power can be improved following the recommendation of section 2.

2. THE BENEFIT OF FREEFORM OPTIMISATION

One of the main advantages of diamond machining is its ability to produce high quality freeform optics. In this section we discuss the benefit of using such surfaces in an integral field unit spectrometer. The architecture of a spectrometer using curved gratings is simple by nature, as it uses a single component (i.e. the freeform grating) to reimage the slit (in the case of a monochromator) or the slice (in the case of Integral Field Spectrometer (IFS)) and disperses the light onto the camera sensor. To compare and assess the improvement in optical quality induced by a different level of surface definition, we model a single mirror spectrograph working in a similar configuration as IGIS.

The optical specifications of IGIS are given in Table 1. The modelling, based on these specifications, is performed with the raytracing package Zemax. Properties such as grating efficiency and relative transmission are not supported by Zemax and will not be studied here. We limit our analysis and discussion to the improvement of geometrical aberrations through the optimisation of spot diagrams. Also, it has to be noted that Zemax does not model gratings as an assembly of blazed segments but as periodic lines. A more in depth analysis using the rigorous coupled-wave analysis (RCWA)⁹ or the C method¹⁰ will have to be used to compute efficiency and spectral noise.

Table 1: IGIS System specifications

slicer dimension (FOV)	4mm x 0.1mm
magnification	0.32
F number	F/9
grating definition	0.15 line / um
wavelength range	400nm - 700nm
Optical path (object)	280mm
off axis angle	8°

In IGIS, the slice object is de-magnified by a factor of 3 by the optics, and the wavelength band is dispersed in the gratings first order. The 4mm x 1.2mm field of view is reformatted into a 2 x 8mm x 0.033mm slit and the [400nm-700nm] waveband is then dispersed over 4mm, leading to an 8 x 4mm image on the detector. To avoid overlap, each image of a slice has been spatially separated from the other, extending slightly the larger dimension by a few millimetres leading to a 12 x 4mm image. Because an Integral field spectrograph slices and reformats a rectangular field into a slit image, each slice works in a slightly different optical configuration to the other. This means that each pupil mirror works with a different off axis angle. The example we have chosen here for our study is representative of an average slice. We have chosen to orientate the line of the grating along the normal to the plane in Fig. 1.

In the simplest case, the grating consists of a tilted sphere. The spot diagram for 3 field positions as well as for the 3 wavelengths is given in Fig. 2(a). The main distortion on the spot diagram is created by astigmatism.¹¹ If the tilted spherical grating is replaced by a tilted ellipse in Fig. 2(b), with the 2 foci located at the centre

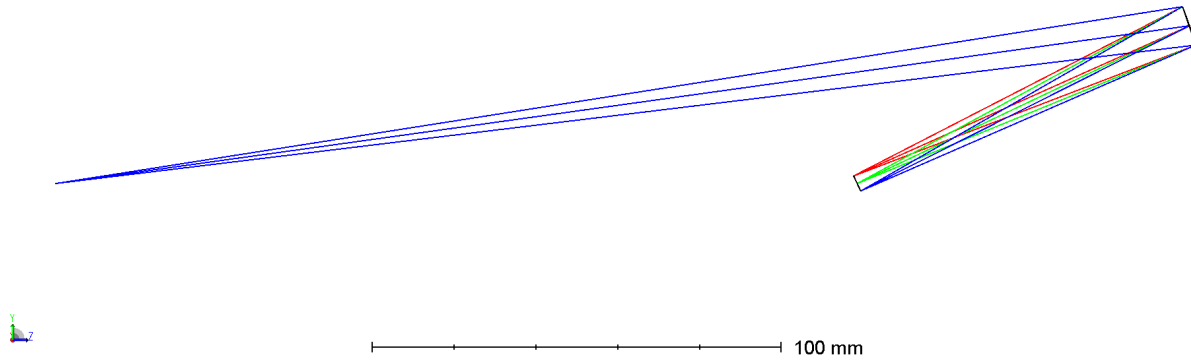


Figure 1: optical configuration use for the simulation. The off axis mirror is either a sphere or an ellipse. The slicer or input slit is on the left.

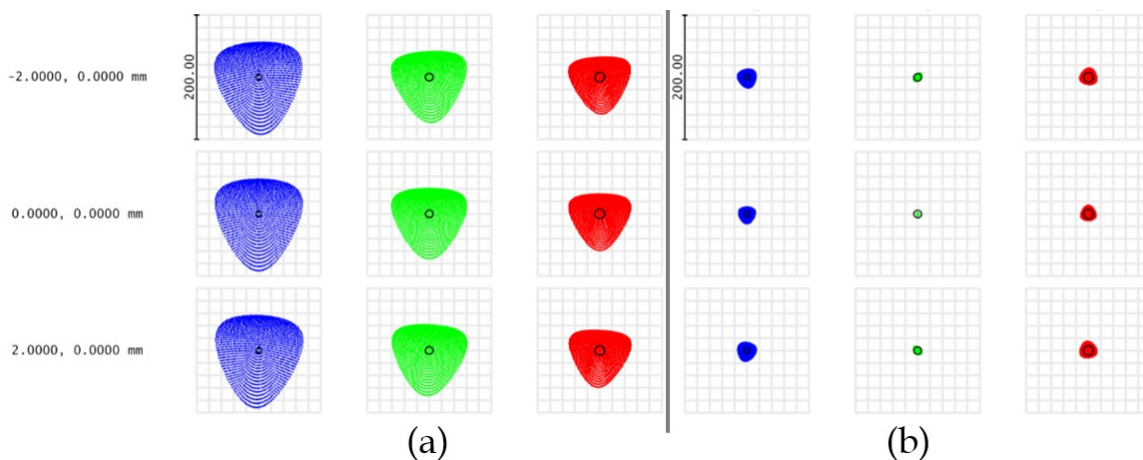


Figure 2: (a) Spot diagram at the image plane of a tilted spherical grating. The RMS spot size is $42 \mu\text{m}$ in average. The colour corresponds to the wavelength, blue is 400nm, green is 550nm and red is 700nm. (b): Spot diagram at the image plane of a tilted elliptical grating. The RMS spot is $7.5 \mu\text{m}$ on average (edge of the field, edge of the spectrum). The ellipse has been optimised for the centre of the field of view (FOV). The black circle corresponds to the Airy disc at the given wavelength.

of the object and image fields, the spot size improves by a factor 5 on average. In the modelling, the elliptical grating is defined by the Zemax surface elliptical grating 1, where the grooves are straight when projected on to the vertex tangent plane. In both cases (for the sphere and the ellipse) the vertex is at the centre of the mirror. The tilt for the ellipse is produced using the first order polynomial coefficients $X0Y1, X1Y0$ and $X1Y1$ in the elliptical grating definition in Zemax.

There is a significant gain in making the shape of the grating a tilted ellipse, and using a 5 axis diamond machine, this comes at no added complexity or cost. As the ellipse is stigmatic for the centre of the FOV, the spot diagram is well below diffraction at the centre of the spectrum and FOV, although a residual astigmatism is visible at the edge.

The next step is to look at quantifying the improvement in the spot size induced by changing the groove period from constant, to linearly variable spaced grooves. Again, the surface is modelled as elliptical grating 1 in Zemax. The gratings spacing is made variable with the dimensionless parameter α according to the equation:

$$\frac{1}{f} = \frac{1}{f_0} + \alpha y, \quad (1)$$

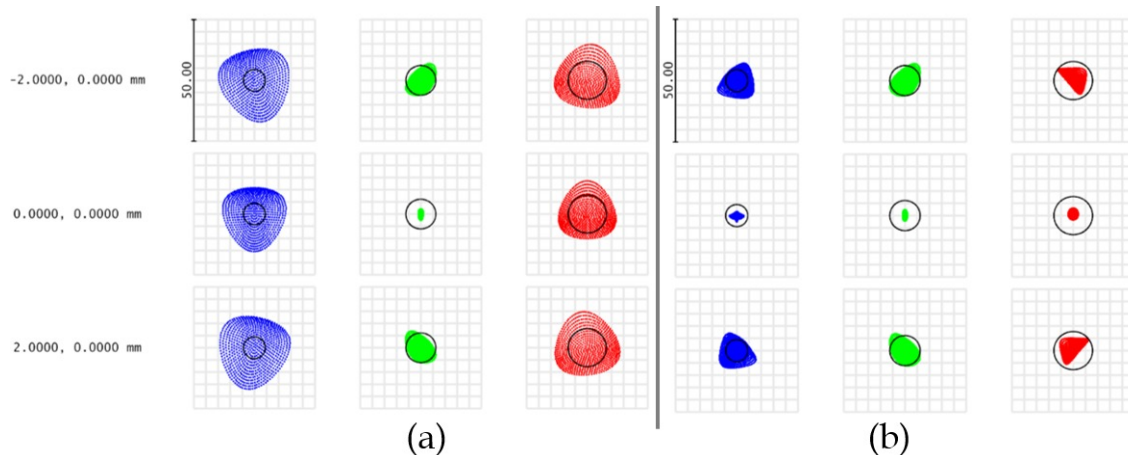


Figure 3: (a) Spot diagram at the image plane of an elliptical grating with constantly spaced grooves. The image is the same as Fig. 2(b), except for the scale which is smaller. The RMS spot radius is $7.5\mu\text{m}$ on average, and the black circle corresponds to the Airy disc at the given wavelength. (b) Spot diagram at the image plane of an elliptical grating with variable spaced grooves. The RMS spot radius is $3.5\mu\text{m}$ RMS on average.

where f is the effective frequency (line per micron), f_0 is the nominal constant frequency (i.e. 0.15 line/micron), and y is the coordinate along the axis normal to the grating line.

The RMS spot size is improved further by a factor 2 or more by making the grating lines linearly spaced. As one can expect, the variable spaced grooves which exclusively affect the spot size along the spectral dimension, have a notable effect in balancing the astigmatism at the corner of the spectrum with respect to the centre (position for which the optimisation has been performed). In the analysis shown in Fig. 3(b), α is 0.0154. This corresponds to a variation in the period between the 2 opposite sides of the grating, (whose diameter is 10mm) equivalent to 150nm.

2.1 The design of IGIS (integrated grating Imaging Spectrograph)

IGIS is the first reported IFS to include an array of curved grating as pupil mirrors. IFS architectures have been discussed in detail here.¹² IFS are usually composed of a mirror slicer whose function is to cut and sample the FOV, a pupil mirror array which re-images the slices and reformats them into a stack to form a long slit, and a slit mirror array whose function is to match the telescope pupil with the spectrographs. In IGIS, the pupil mirrors also act as the spectrograph's grating, so there is no need for slit mirrors. Therefore, the detector is placed in the image plane. IGIS system specifications have been given in Tab. 1 and the optical layout is represented in Fig. 4. The incoming light enters the system via a first optics in (1), which creates an image in the slicer plane. The aperture stop is placed on this first lens. The light is redirected towards the slicer via a folding mirror (2). The slicer is composed of 2 sets of 6 slices, dimension (4mm x 0.1mm). Each set of 6 slices readdresses the light either towards the left or right arm, while reimaging the system's pupil onto the pupil mirror (6), via 2 folding mirrors (4) and (5). On each arm, the pupil mirrors are freeform gratings, with the groove orientated vertically (parallel to the slices). The spectrum is finally imaged onto the detector (8) via a folding mirror (7). The system is composed of 2 identical and symmetrical arms.

IGIS is a highly compact design, and has an overall dimension of 240 x 183 x 84mm. If the pupil mirrors are machined on their final position and fixture, the tight arrangement is a challenge in terms of machining as the tool path sometimes extends beyond the optical surface and the tool can collide into the neighbouring mirror. The machining process consists of two steps. The first step is to get the substrate form as close as possible to the final shape, and the second step is to machine the grooves. It is of course important to remove most of the material during step 1, so as to maximise the lifetime of the diamond tool used for machining the grooves. For the first step, if the mirrors were to be turned, one strategy would entail splitting the array into a single unit and machining the mirror either independently, as an on-axis sphere with slow tool servo, or by turning them off axis after repositioning all the mirrors on a fixture in a rearranged configuration. Those 2 options have the drawback

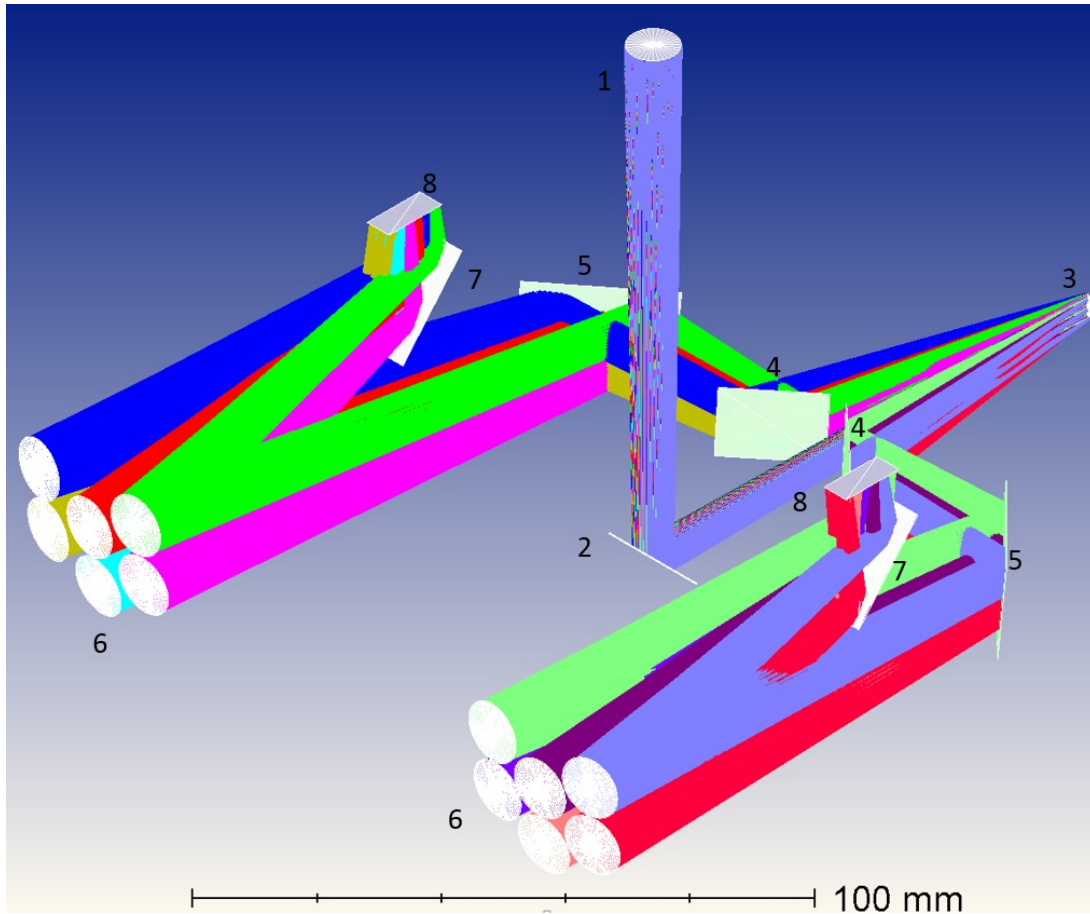


Figure 4: IGIS layout. The description of the beam path is given in the text. The beam going onto each slice is represented by a different colour.

of increasing the complexity in the design, or the assembly and most importantly reducing the accuracy in the mirror to mirror positional registration. Among the few machining options, the strategy that was favoured and subsequently implemented in a test, was to diamond mill an array of 3 mirrors on their final fixture, prior to machining the grooves. The test that was undertaken was performed on a RSA 6061 blank, whose dimension and shape were similar to IGIS pupil mirrors. Fig. 5 shows the test blank with 3 off-axis sphere. The advantage of diamond milling, compared to turning for this particular configuration is that it enables an extremely high registration of the surfaces with one another as the array can be machined directly on its final fixture. With that in mind, each mirror in IGIS is equipped with a 2 pins interface which guarantees that each mirror can be removed and repositioned onto the fixture with an optimal accuracy. Each mirror can then be milled in situ, with the adjacent mirror removed.

The machining of the groove has not been tested yet and will be reported in future publications. A blazed angle needs to remain constant from groove to groove independently from the position on the surface. This is possible with the use of the B axis, whose rotation compensates for the local gradient on the surface. Therefore, as the tool is sequentially moved from groove to groove, it is also subjected to a small rotation (matching the local gradient variation), keeping the blazed angle constant.

3. POSSIBLE DESIGN IMPROVEMENT

We have seen in the section 2 that a tilted elliptical grating can improve the spot diagram by a factor of 5 compare to spherical gratings. In this section, we compare 2 potentials designs for IGIS, one with tilted spheres and the other with tilted ellipses for the shape of the grating, and study how the resolving power can be affected.

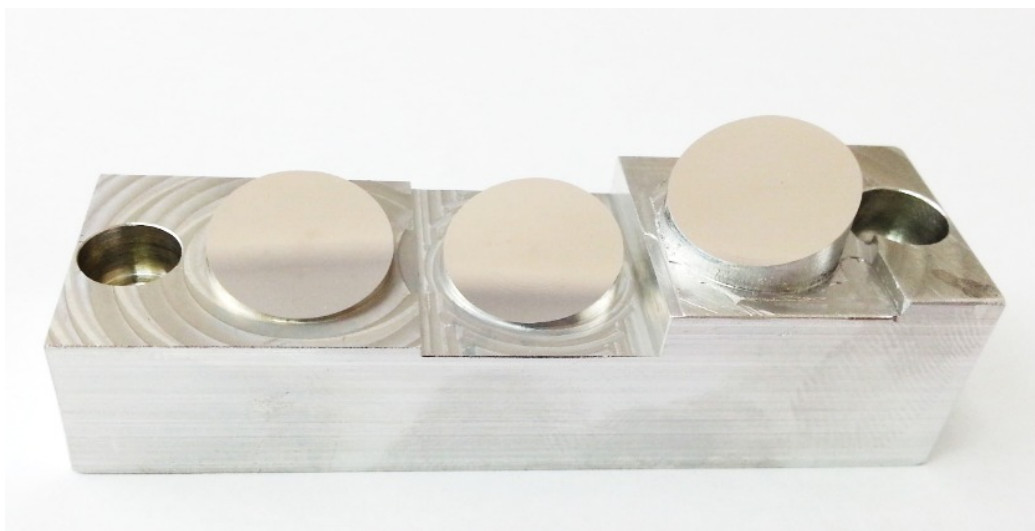


Figure 5: Diamond milling test on a blank representative of the pupil mirrors in IGIS, with similar size, tilt and radius of curvature.

The spot diagram for 9 positions in the full FOV (4mm x 11.5mm) is given in Fig. 6. The colour is coded by wavelength, with the blue, green and red respectively referring to 400nm, 550nm and 700nm. For a design based on spherical mirror gratings, on Fig. 6(a), the spectrograph resolving power is $R = 100$ and is mainly limited by astigmatism (as discussed in section 2). As each pupil mirror works at a different tilt from the others, the spots do not keep the same shape from slice to slice. The average spot size is $70 \mu\text{m}$ RMS. On 6(b), the spots diagrams are given for a design based on an elliptical grating, for the same position in the field of view as previously. The average spot size is $14 \mu\text{m}$ RMS corresponding to the same ratio of improvement as discussed in the first section. The central spot is the reference spot on which the optimisation has been performed. It is interesting to note that, due to the rays angle of incidence at the edge of the spectrum, the spot diagram becomes stretched. If the imaging plane was normal to the chief ray, the spots would be similar to those on Fig. 3, but because of the incidence, the 3D spot is projected onto the imaging plane and produces the elongation. The gain in optical quality offered by elliptical gratings in IGIS is actually not required for its operational conditions, and spots with a size similar to those obtained with the spherical gratings are sufficient to meet the system requirement. However, the discussion about possible improvements is interesting and can be relevant for future designs. Also, because the pupil mirrors are the only components with optical power in the system, the pupil mirror block can be upgraded to an array of elliptical gratings later on.

The variability in the spacing between the gratings grooves has also been investigated but no noticeable improvement has been obtained. The reason is that the spot size remains predominantly limited by the effect on the spot of the chief rays high angle of incidence. Finally, on Fig. 7, the full field spot size is given at the detector plane in the case of spherical or elliptical gratings. The resolving power, which is 100 on the left, can be improved up to 500 on the right.

4. CONCLUSION

Multi-axis diamond machining is shown to be a key modality for the manufacturing of curved blazed gratings and their implementation in the next generation of compact, high performance IFS. The gratings form and period can be optimised by the optical engineer to significantly improve the system resolving power. We have presented IGIS, which is a first IFS which uses an array of freeform gratings to reformat and disperse the light sampled by a slicer. An important advantage offered by multi-axis diamond machining is that the multiple surfaces can be machined on their final fixture keeping an optimal registration between them, limited only by the positional submicron accuracy of the machine and the residual axis non-orthogonality. These 2 errors can be nonetheless independently calibrated and corrected for. A test on a blank similar in size and shape to the pupil mirrors of IGIS has been produced and confirmed that diamond milling can be successfully used to pre-machine and potentially finish (if no grating is needed) each pupil mirror in a compact assembly.

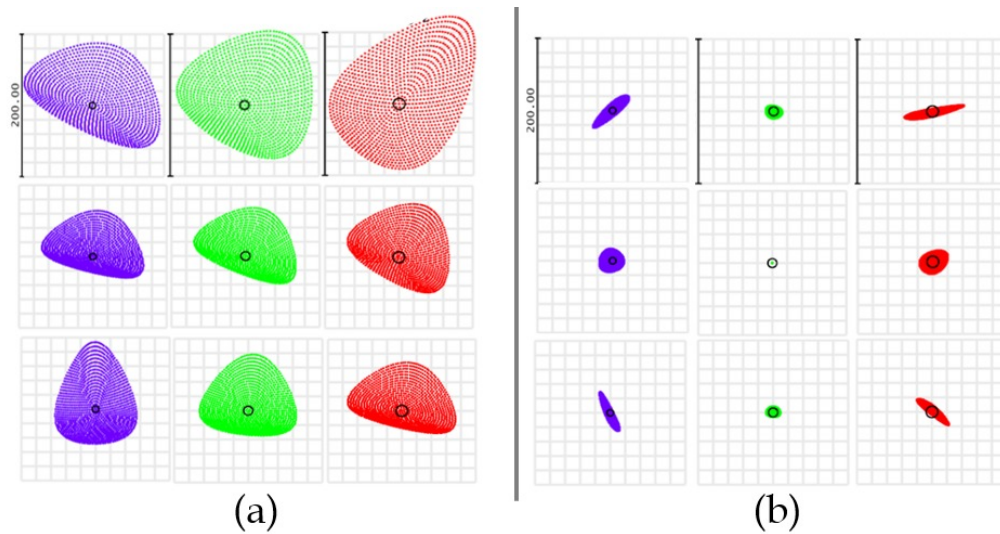


Figure 6: (a) Spot diagram with spherical grating; (b) Spot diagram with elliptical grating and constant groove spacing.

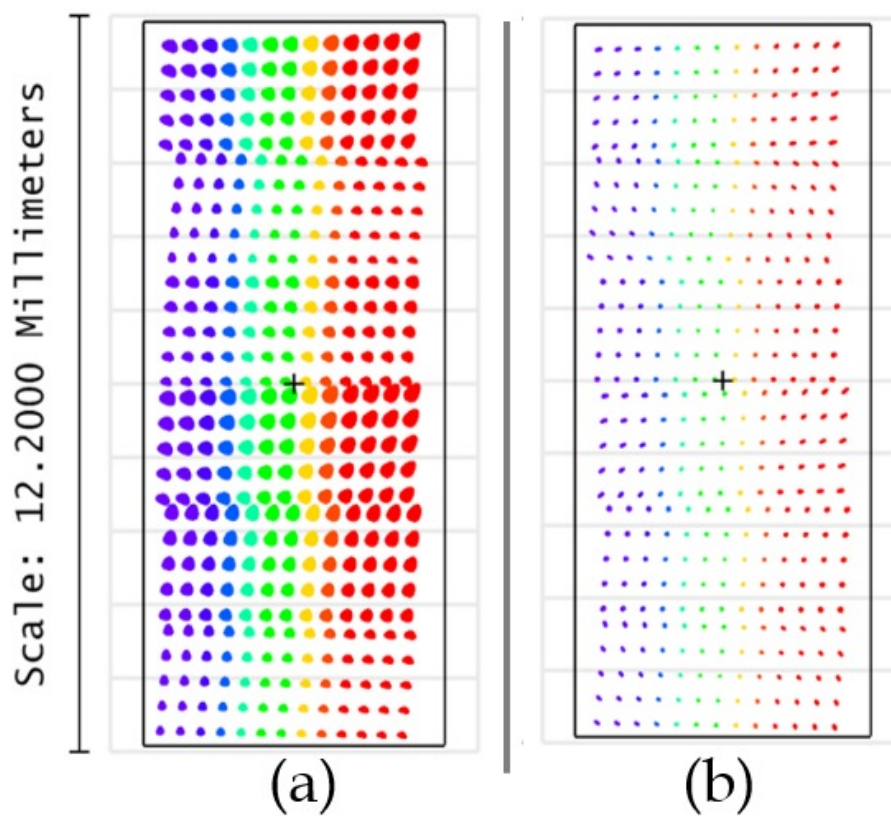


Figure 7: Full FOV spot diagram for a design with a spherical grating (a) or for a design with elliptical grating (b).

Acknowledgements

Thank you to Anthony Lucien for his help in the mechanical design of the assembly.

REFERENCES

1. M. Singh, "New monochromators of concave grating suitable for space telescopes," *Appl. Opt.* **17**, pp. 1815–1823, Jun 1978.
2. J. F. Wu, Y. Y. Chen, and T. S. Wang, "Flat field concave holographic grating with broad spectral region and moderately high resolution," *Appl. Opt.* **51**, pp. 509–514, Feb 2012.
3. A. B. Shafer, L. R. Megill, and L. Droppleman, "Optimization of the Czerny–Turner spectrometer*," *J. Opt. Soc. Am.* **54**, pp. 879–887, Jul 1964.
4. P. Mouroulis, D. W. Wilson, P. D. Maker, and R. E. Muller, "Convex grating types for concentric imaging spectrometers," *Appl. Opt.* **37**, pp. 7200–7208, Nov 1998.
5. Y. Aoyagi, K. Sano, and S. Namba, "High spectroscopic qualities in blazed ion-etched holographic gratings," *Optics Communications* **29**(3), pp. 253 – 255, 1979.
6. E. W. Palmer, M. C. Hutley, A. Franks, J. F. Verrill, and B. Gale, "Diffraction gratings (manufacture)," *Reports on Progress in Physics* **38**(8), p. 975, 1975.
7. B. Guldemann, A. Deep, and R. Vink, "Overview on grating developments at ESA," *CEAS Space Journal* **7**(4), pp. 433–451, 2015.
8. J. M. Cobb, L. E. Comstock, P. G. Dewa, M. M. Dunn, and S. D. Flint, "Advances in diamond-turned surfaces enable unique cost-effective optical system solutions," 2006.
9. M. G. Moharam, T. K. Gaylord, E. B. Grann, and D. A. Pommet, "Formulation for stable and efficient implementation of the rigorous coupled-wave analysis of binary gratings," *J. Opt. Soc. Am. A* **12**, pp. 1068–1076, May 1995.
10. L. Li, J. Chandezon, G. Granet, and J.-P. Plumey, "Rigorous and efficient grating-analysis method made easy for optical engineers," *Appl. Opt.* **38**, pp. 304–313, Jan 1999.
11. C. H. F. Velzel, "A general theory of the aberrations," *J. Opt. Soc. Am.* (4), pp. 346–353.
12. R. C. Jeremy Allington-Smith, "Sampling and background subtraction in fiber lenslet integral field spectrographs," *Publications of the Astronomical Society of the Pacific* **110**(752), pp. 1216–1234, 1998.